Datasets of three non-equilibrium pressure gradient turbulent boundary layers

Taygun R. Gungor, Ayse G. Gungor, Yvan Maciel

Thursday 22nd February, 2024

We present three DNS datasets in this report, all generated using Direct Numerical Simulation (DNS). Relevant information about the code and computational setup can be found in the papers of Simens et al. (2009), Borrell et al. (2013), Sillero (2014), Gungor et al. (2016). The three datasets discussed here are highly non-equilibrium turbulent boundary layers developing under a pressure gradient. We depict the flow development for all cases, illustrating the evolution of the outer and inner pressure gradient parameters in accordance with the paper of Gungor et al. (2024), along with the shape factor and skin friction coefficient. Additionally, we select several streamwise positions based on the shape factor to provide a more detailed perspective. In this report, we present figures of various variables, including the inner-scaled and outer-scaled mean velocities, and Reynolds stresses at these chosen streamwise positions. The figures and tables can be found on the following pages. Furthermore, the raw data presented in this report, along with other relevant variables, can be accessed on the following websites:

- https://yvanmaciel.gmc.ulaval.ca/databases/
- http://web.itu.edu.tr/gungoray/databases/

For proper citation, kindly refer to the papers listed below when utilizing the datasets. It is crucial to note that there might be minor variations between the data presented in the referenced papers and the data presented here due to our utilization of different definitions. The boundary layer thickness is computed using the method outlined by Griffin et al. (2021). The edge velocity is considered to be the velocity at the position of the boundary layer edge. Furthermore, we employ the definitions provided in equations 8 and 9 for the pressure gradient parameters. In addition, the free-stream velocity at the inlet is 1. The definitions are given below.

$$\begin{aligned} U =& \langle u' \rangle, u = u' - U \\ V =& \langle v' \rangle, v = v' - V \\ W =& \langle w' \rangle, w = w' - W \end{aligned} \tag{1}$$

$$\begin{aligned} u2 =& \langle uu \rangle \\ v2 =& \langle vv \rangle \\ w2 =& \langle ww \rangle \\ uv =& \langle uv \rangle \end{aligned} \tag{2}$$

$$\begin{aligned} \delta = y \ \mid \ at \ \ U = 0.99 \times U_{inviscid} \\ U_e = U \ \mid \ at \ \ y = \delta \end{aligned} \tag{3}$$

$$C_f = \frac{\tau_w}{0.5 \rho U_e^2} \tag{4}$$

$$H = \delta^* / \theta \tag{5}$$

$$\begin{aligned} Re_\tau &= \delta u_\tau / \nu \\ Re_\theta &= \theta U_e / \nu \end{aligned} \tag{6}$$

$$\beta_{RC} = \frac{\delta^*}{\rho U_\tau^2} \frac{dp_e}{dx} \tag{7}$$

$$\beta_{ZS} = \frac{\delta}{\rho U_{ZS}^2} \frac{dp_e}{dx} \tag{8}$$

$$\beta_i = \frac{\nu}{\rho u_\tau^3} \frac{dp_w}{dx} \tag{9}$$

where u', v' and w' are the instantaneous velocities in the streamwise, wall-normal, and spanwise directions, $\langle . \rangle$ indicates the temporal and spanwise averaging, $U_{inviscid}$ is the inviscid mean streamwise velocity approximation computed with the method of Griffin et al. (2021), δ is the boundary layer thickness, δ^* is the displacement thickness, θ is the momentum thickness, DOI is the domain of interest (useful domain), ρ is density, U_{ZS} is the Zagorola-Smits velocity, p_e is the pressure at the edge of boundary layer, ν is viscosity, u_τ is the friction velocity, p_w is the pressure at the wall and x is the streamwise direction. In addition to these, δ_{av} is the average boundary layer thickness in the useful domain.

DNS16: Gungor, A. G., Maciel, Y., Simens, M. P., & Soria, J. (2016). Scaling and statistics of large-defect adverse pressure gradient turbulent boundary layers. *International Journal of Heat and Fluid Flow*, 59, 109-124.

DNS22: Gungor, T. R., Maciel, Y., & Gungor, A. G. (2022). Energy transfer mechanisms in adverse pressure gradient turbulent boundary layers: production and inter-component redistribution. *Journal of Fluid Mechanics*, 948, A5.

DNS23: Gungor, T. R., Gungor, A.G., & Maciel, Y. (2024). Turbulent boundary layer response to uniform changes of the pressure force contribution. arXiv preprint arXiv:2402.13067

References

Simens, M.; Jiménez, J.; Hoyas, S.; Mizuno, Y. A high-resolution code for turbulent boundary layers. *Journal of Computational Physics* **2009**, *228*, 4218–4231.

Borrell, G.; Sillero, J.; Jiménez, J. A code for direct numerical simulation of turbulent boundary layers at high Reynolds numbers in BG/P supercomputers. *Computers & Fluids* **2013**, *80*, 37–43.

Sillero, J. High Reynolds numbers turbulent boundary layers. Ph.D. thesis, Universidad Politécnica de Madrid, 2014.

Gungor, A.; Maciel, Y.; Simens, M.; Soria, J. Scaling and statistics of large-defect adverse pressure gradient turbulent boundary layers. *International Journal of Heat and Fluid Flow* **2016**, *59*, 109–124.

Gungor, T.; Gungor, A.; Maciel, Y. Turbulent boundary layer response to uniform changes of the pressure force contribution. *arXiv preprint arXiv:2402.13067* **2024**,

Griffin, K.; Fu, L.; Moin, P. General method for determining the boundary layer thickness in nonequilibrium flows. *Physical Review Fluids* **2021**, *6*, 024608.

Gungor, T.; Maciel, Y.; Gungor, A. Energy transfer mechanisms in adverse pressure gradient turbulent boundary layers: production and inter-component redistribution. *Journal of Fluid Mechanics* **2022**, *948*, A5.

Gungor, T.; Maciel, Y.; Gungor, A. Turbulent activity in the near-wall region of adverse pressure gradient turbulent boundary layers. *arXiv preprint arXiv:1409.0473* **2024**,

DNS 16

Position	x/δ_{avg}	H	$C_f \times 1000$	Re_τ	Re_θ	β_{ZS}	β_i	β_{RC}
S1	2.84	1.50	3.58044	444	1238	0.472	0.0186	1.39
S2	4.66	1.60	2.78789	452	1614	0.524	0.0378	3.19
S3	7.78	2.00	1.21794	395	2541	0.304	0.1247	12.06
S4	8.54	2.16	0.89940	369	2794	0.247	0.1741	16.88
S5	9.86	2.50	0.46812	302	3176	0.159	0.3428	31.22
S6	11.11	2.87	0.20119	224	3493	0.105	0.8547	64.42
S7	11.54	3.00	0.14780	200	3578	0.091	1.1881	82.74
S8	13.06	3.43	-0.00179	25	3849	0.062	612.5601	5776.35

Table 1: Stations S3, S5, S7 and S8 are those employed in Gungor et al. (2016). However, because we now compute the boundary layer thickness using the method of Griffin et al. (2021), the values of all the parameters in the table, except β_i, have changed slightly. Note also that the definition of β_{ZS} differs from the one used in Gungor et al. (2016). δ_{avg} for DNS16 is 7.83.

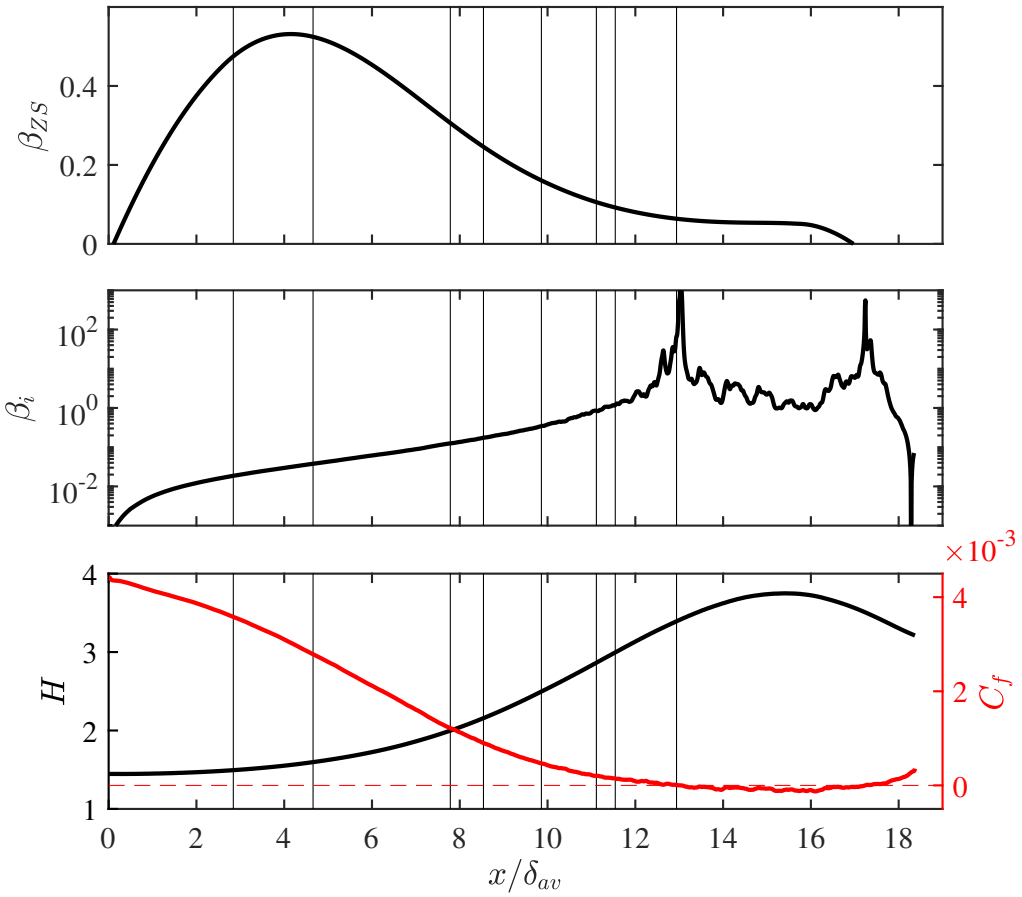

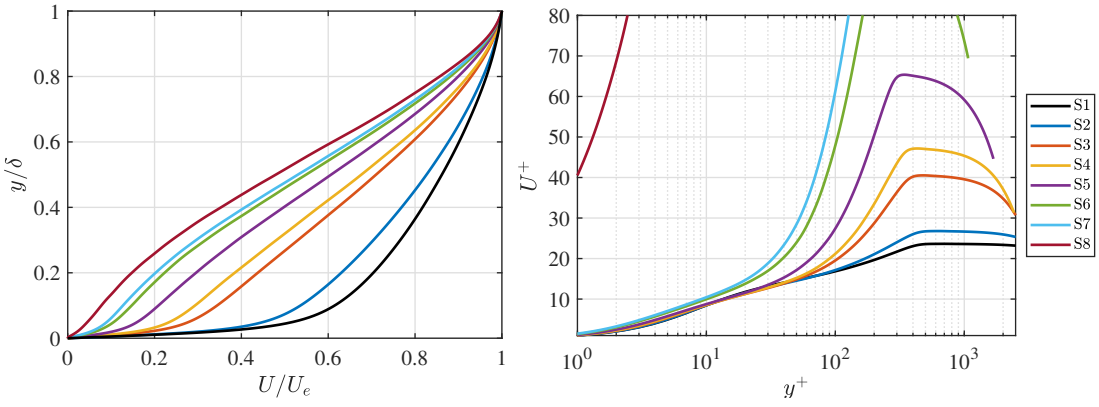

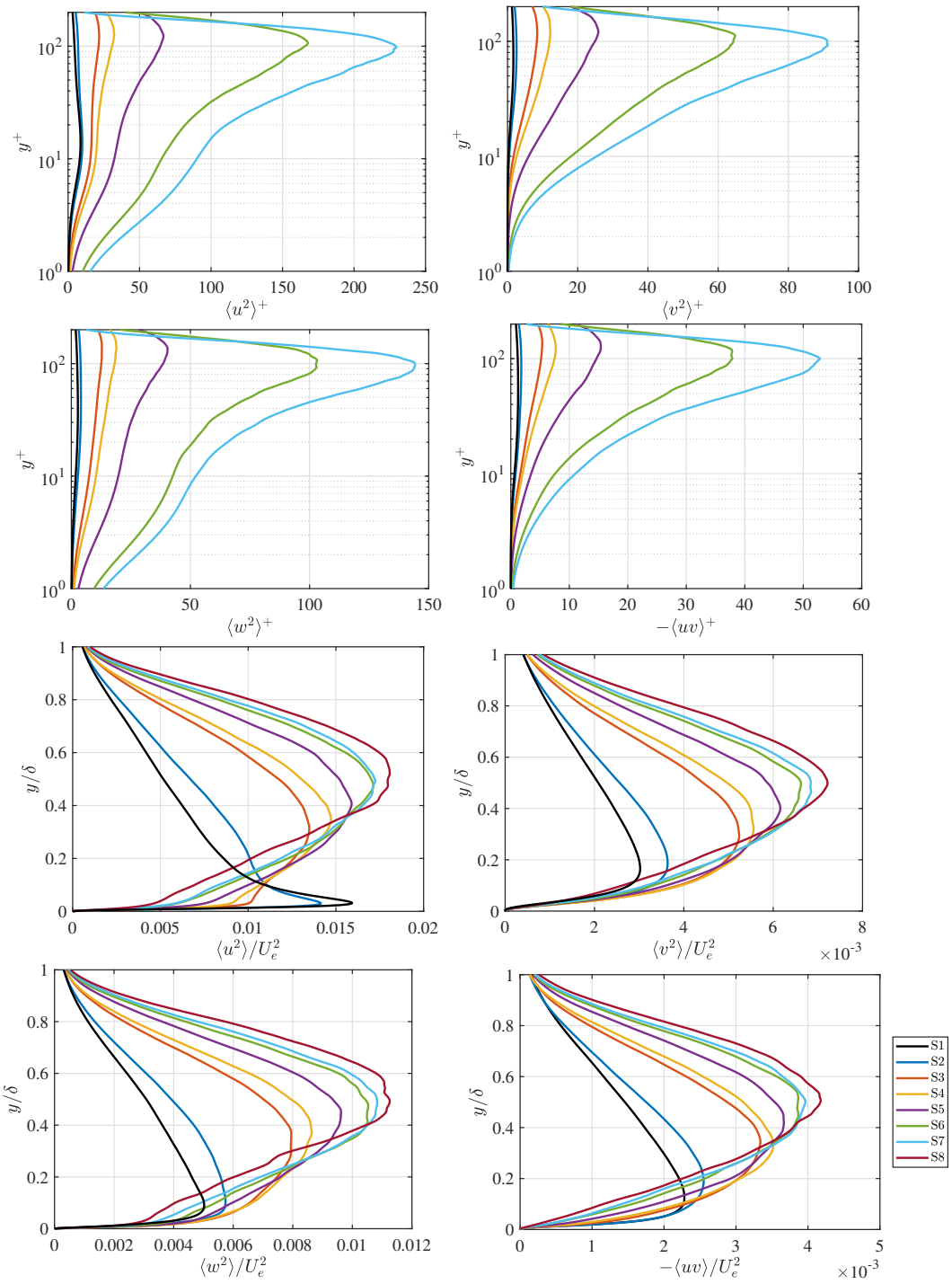
y^+
$\langle u^2\rangle^+$
$\langle v^2\rangle^+$
$\langle w^2\rangle^+$
$-\langle uv\rangle^+$
y/δ
$\langle u^2\rangle/U_e^2$
$\langle v^2\rangle/U_e^2$
$\langle w^2\rangle/U_e^2$
$-\langle uv\rangle/U_e^2$
$\times 10^{-3}$
S1
S2
S3
S4
S5
S6
S7
S8

DNS 22

Position	x/δ_{avg}	H	$C_f \times 1000$	Re_τ	Re_θ	β_{ZS}	β_i	β_{RC}
S1	3.26	1.50	3.05665	642	2066	0.373	0.0135	1.53
S2	5.88	1.66	2.17187	649	2892	0.332	0.0278	3.68
S3	7.93	1.85	1.48510	627	3686	0.243	0.0460	6.62
S4	10.20	2.16	0.85675	571	4615	0.156	0.0831	12.34
S5	12.25	2.50	0.46263	497	5411	0.102	0.1526	21.63
S6	13.01	2.64	0.35988	464	5674	0.087	0.1964	26.67
S7	14.34	2.87	0.22328	403	6101	0.069	0.3266	39.94
S8	16.04	3.13	0.12597	336	6575	0.056	0.6301	67.00

Table 2: Stations S2 and S6 are those employed in Gungor et al. (2022). However, because we now compute the boundary layer thickness using the method of Griffin et al. (2021), the values of all the parameters in the Table, except β_i, have changed slightly. δ_{avg} for DNS16 is 13.71.

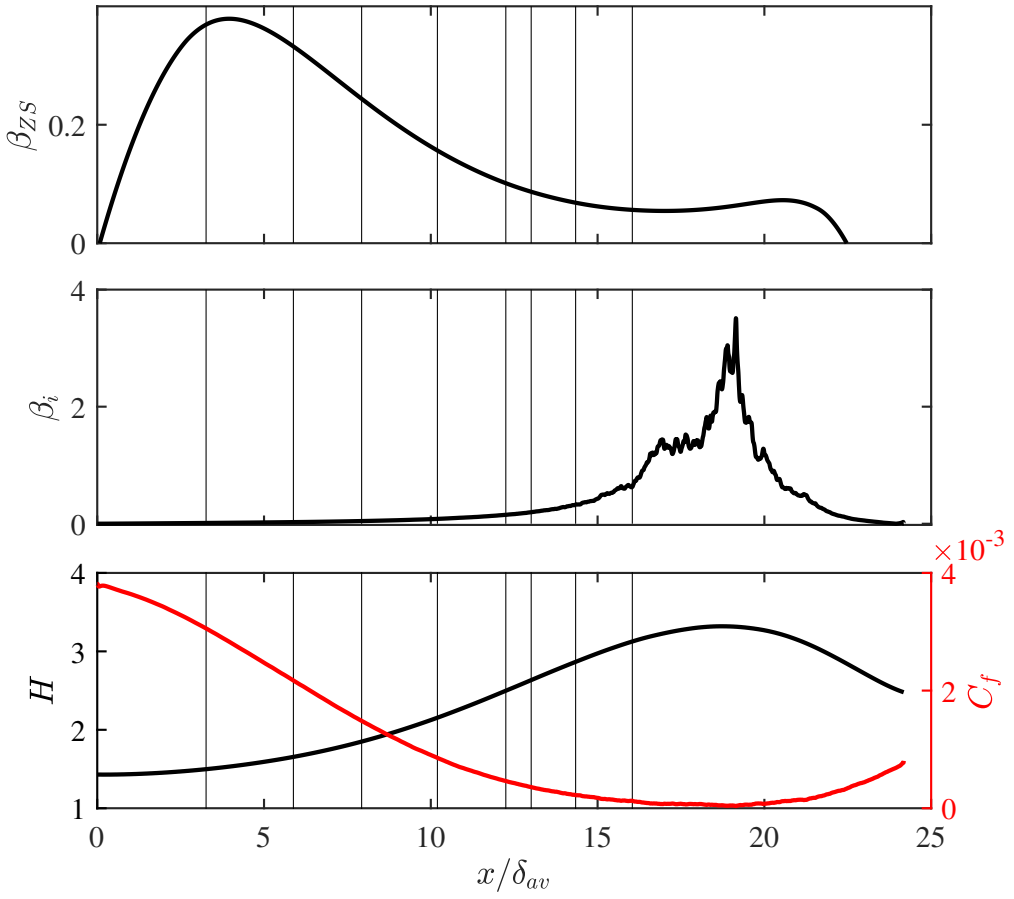

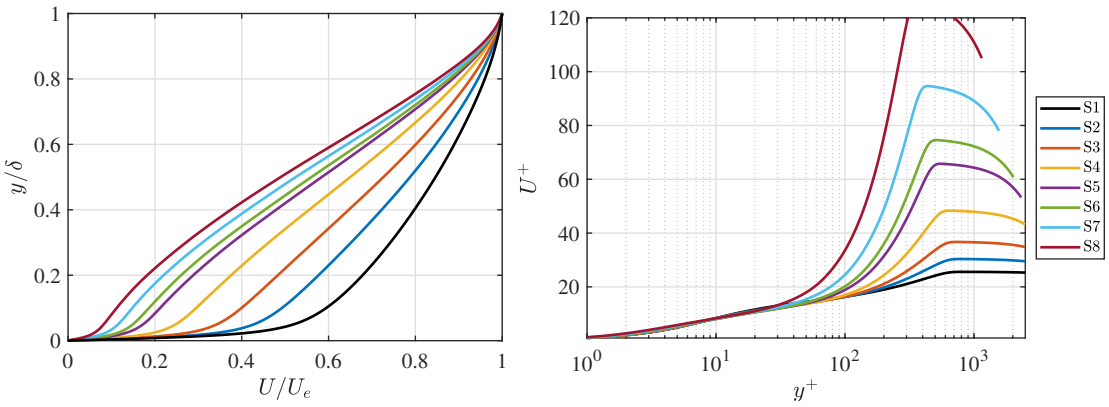

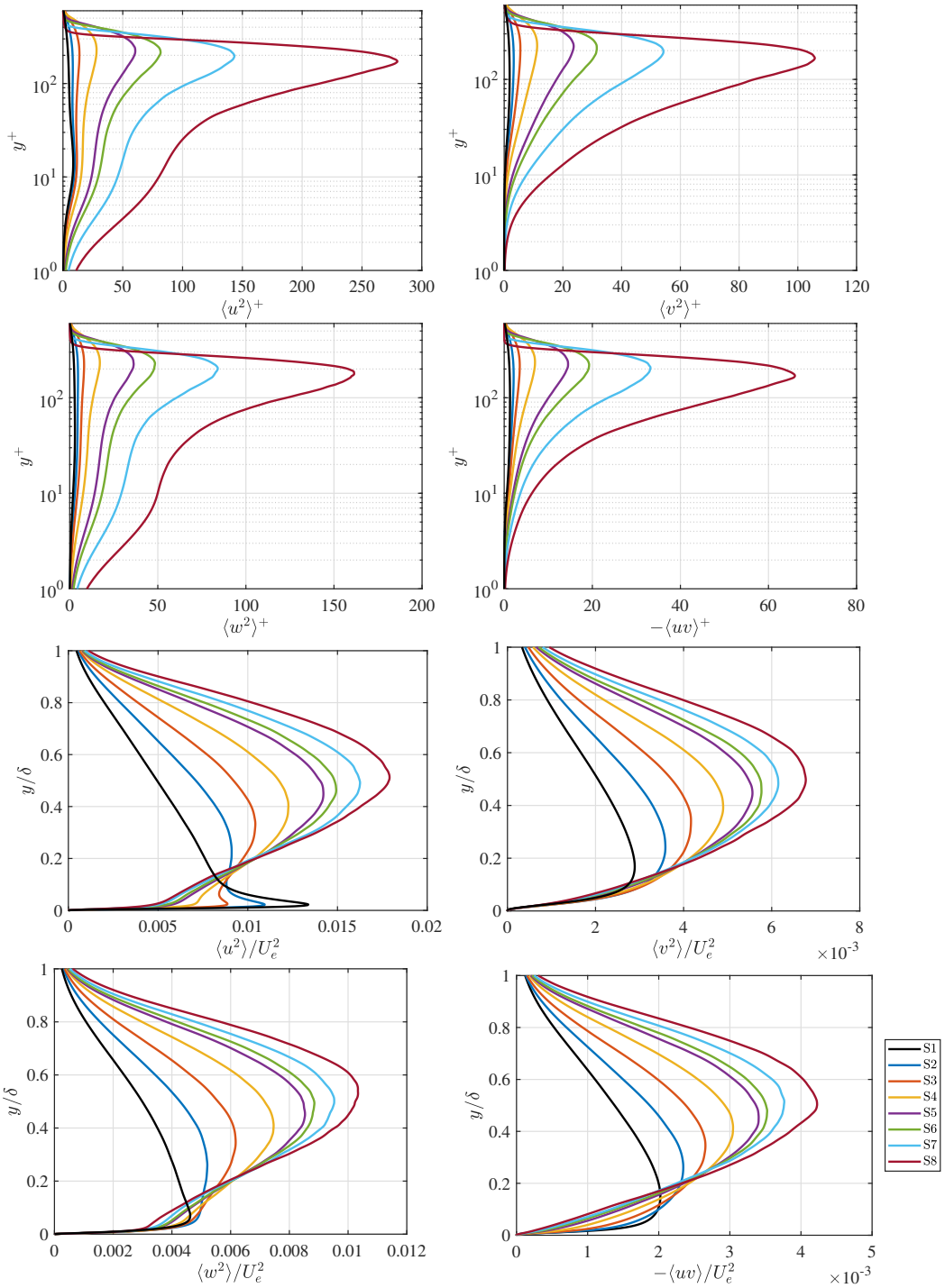
y^+
$\langle u^2\rangle^+$
$\langle v^2\rangle^+$
$\langle w^2\rangle^+$
$-\langle uv\rangle^+$
y/δ
$\langle u^2\rangle/U_e^2$
$\langle v^2\rangle/U_e^2$
$\langle w^2\rangle/U_e^2$
$-\langle uv\rangle/U_e^2$
$\times 10^{-3}$
S1
S2
S3
S4
S5
S6
S7
S8

DNS 23

Position	x/δ_{avg}	H	$C_f \times 1000$	Re_τ	Re_θ	β_{ZS}	β_i	β_{RC}
S1	3.92	1.41	3.38462	856	2421	0.084	0.0016	0.22
S2	11.92	1.60	2.03336	1058	4849	0.328	0.0168	3.41
S3	16.61	2.16	0.68652	884	7918	0.179	0.0729	17.05
S4	19.42	2.65	0.29354	714	9593	0.090	0.1575	33.15
S5	22.34	2.88	0.22488	721	10909	0.054	0.1607	30.38
S6	25.43	2.65	0.40239	1025	12036	0.036	0.0476	9.84
S7	29.14	2.16	0.86579	1524	12707	0.001	0.0028	0.05
S8	35.22	1.60	1.89861	2334	12004	-0.189	-0.0051	-2.05

Table 3: These stations are those employed in Gungor et al. (2024). However, because we here compute the boundary layer thickness using the method of Griffin et al. (2021), the values of all the parameters in the Table, except β_i, have changed slightly. δ_{avg} for DNS16 is 21.87.

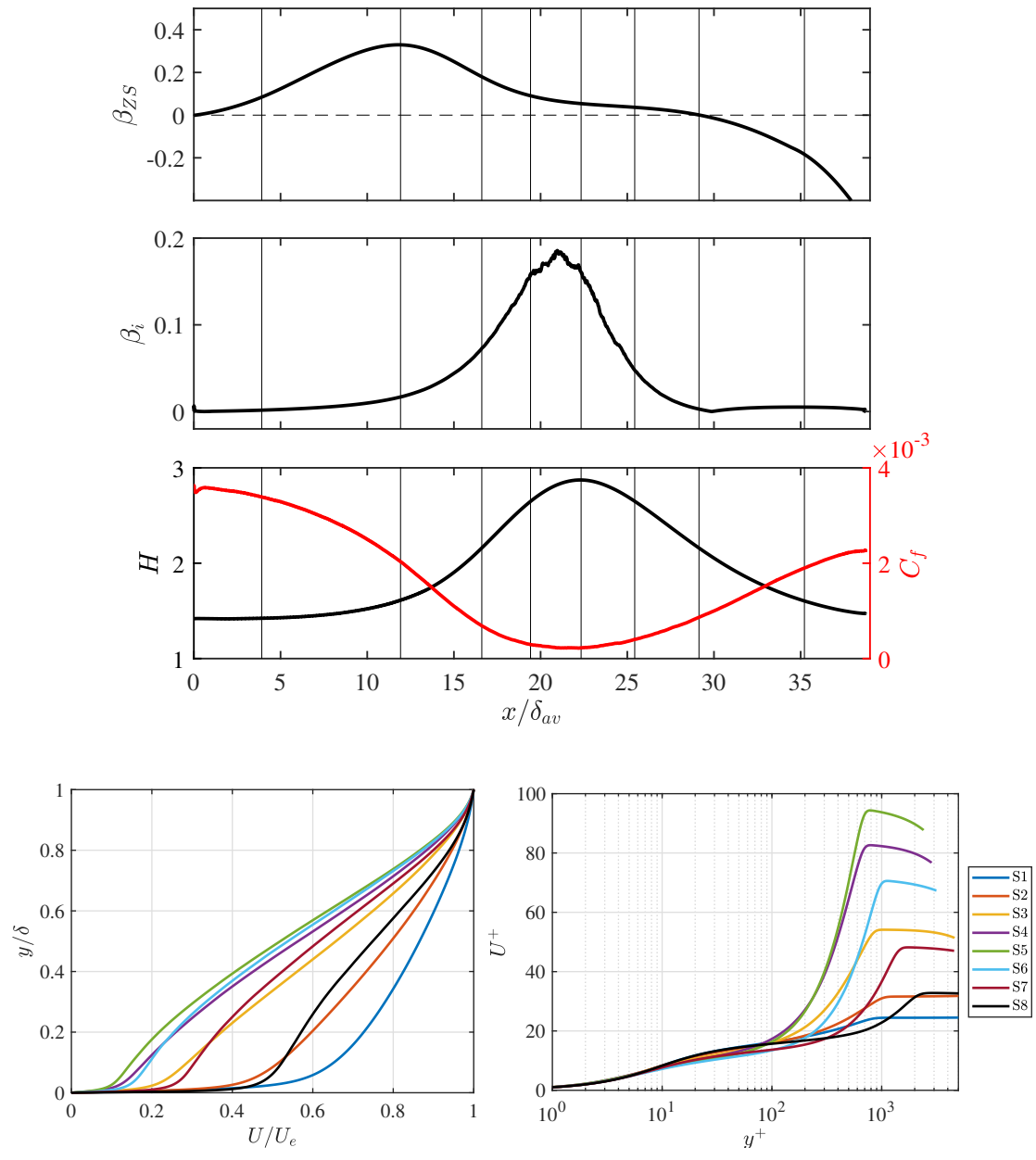

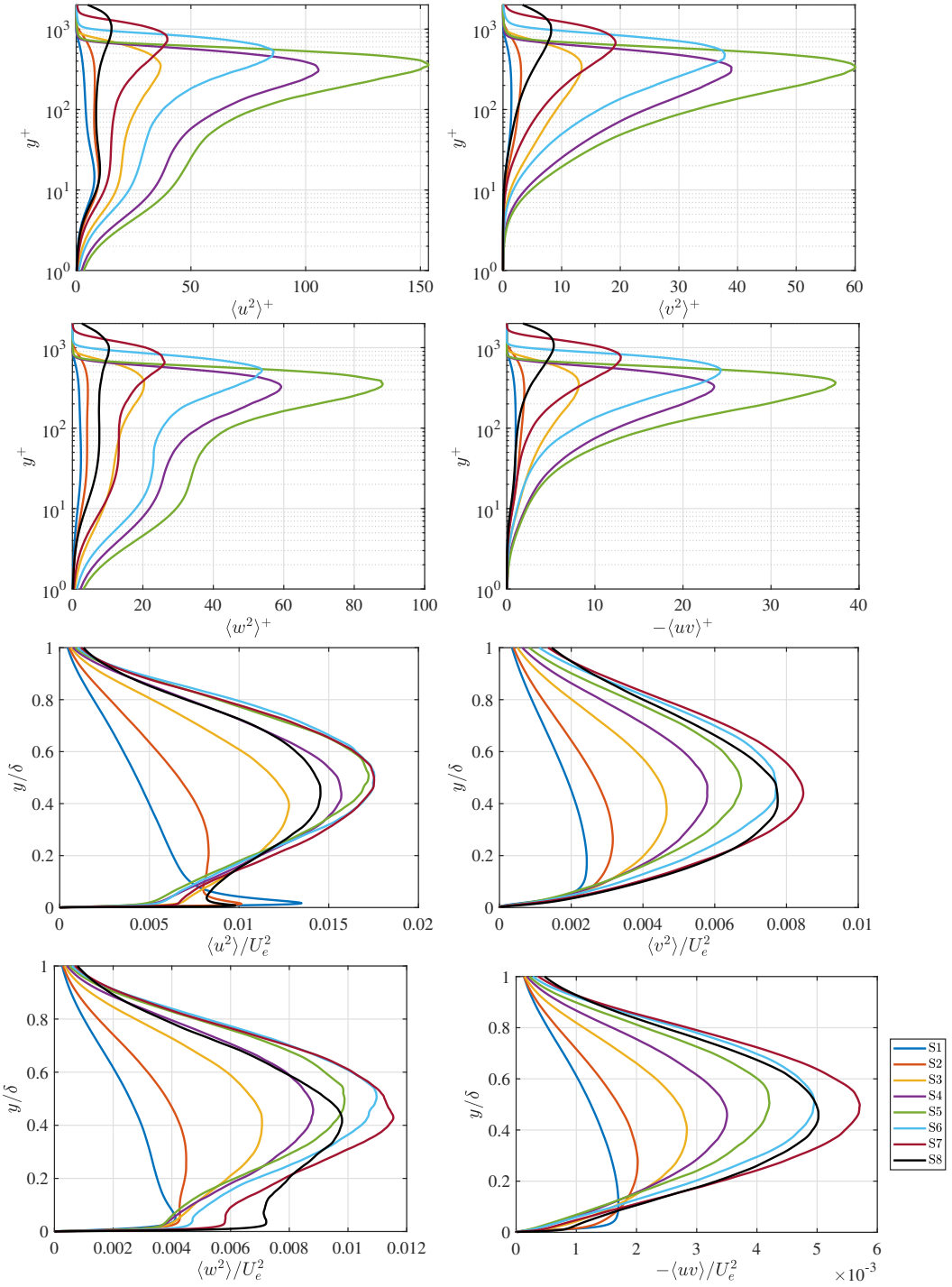
y^+
$\langle u^2\rangle^+$
$\langle v^2\rangle^+$
$\langle w^2\rangle^+$
$-\langle uv\rangle^+$
y/δ
$\langle u^2\rangle/U_e^2$
$\langle v^2\rangle/U_e^2$
$\langle w^2\rangle/U_e^2$
$-\langle uv\rangle/U_e^2$
$\times 10^{-3}$
S1
S2
S3
S4
S5
S6
S7
S8